Click Here for Full Article

Abrupt wind regime changes in the North Atlantic Ocean during the past 30,000–60,000 years

Constancia López-Martínez,[1] Joan O. Grimalt,[1] Babette Hoogakker,[2] Jens Gruetzner,[3] Maryline J. Vautravers,[2,4] and I. Nicholas McCave[2]

[1] The inputs of higher plants in Blake Outer Ridge (subtropical western North Atlantic) during marine isotope stage 3 (MIS3) have been recorded at high resolution by quantification of $C_{23}-C_{33}$ odd carbon numbered n-alkanes and $C_{20}-C_{30}$ even carbon numbered n-alkan-1-ols in sediment sections of Ocean Drilling Program Site 1060. The changes of these proxies at this open marine site are mainly related to eolian inputs. Their concentrations and fluxes exhibit major abrupt variations that are correlated with Dansgaard/Oeschger (D/O) patterns in Greenland ice cores. The ratios between interstadials and stadials range between 2 and 9 times. The intense flux increases in the D/O stadials are linked to strong enhancements of the westerly wind regime at these subtropical latitudes during stadials. The observed variation was paralleled by changes in wind-blown dust and the polar circulation index in Greenland ice, which is in agreement with previously hypothesized atmospheric teleconnections between northern and middle-low latitudes of the Northern Hemisphere. The close correspondence between sedimentary and ice core proxies is evidence that crossings of the glacial climate thresholds involved major reorganizations of the troposphere. The observed large rise in higher plant biomarkers indicates that climate stabilization in the D/O stadial conditions led to main increases in wind intensity.

Citation: López-Martínez, C., J. O. Grimalt, B. Hoogakker, J. Gruetzner, M. J. Vautravers, and I. N. McCave (2006), Abrupt wind regime changes in the North Atlantic Ocean during the past 30,000–60,000 years, *Paleoceanography*, *21*, PA4215, doi:10.1029/2006PA001275.

1. Introduction

[2] The Earth's climate fluctuates between different steady state modes that are defined by sensitive thresholds [*Broecker*, 1997; *Ganopolski and Rahmstorf*, 2001]. During the last glacial crossing over these limits involved abrupt climate transitions in the Arctic regions (defined as Dansgaard-Oeschger stadials and interstadials (D/O) and Heinrich events (HE)) [*Heinrich*, 1988; *Bond et al.*, 1993; *Dansgaard et al.*, 1993]. These transitions were generally recorded in the Northern Hemisphere by rapid changes of sea surface temperature [*Cacho et al.*, 1999; *McManus et al.*, 1999], continental vegetation [*Allen et al.*, 1999; *Sánchez Goñi et al.*, 2002] and humidity [*Wang et al.*, 2001].

[3] While most North Atlantic paleoceanographic and paleoclimatic studies covering the last glacial are centered in the northern and eastern part (see reviews by *Leuschner and Sirocko* [2000], *Voelker and Workshop Participants* [2002], and *Rohling et al.* [2003]), less attention has been paid to the western midlatitudes [*Keigwin and Jones*, 1994; *Keigwin and Boyle*, 1999; *Hagen and Keigwin*, 2002; *Vautravers et al.*, 2004]. In this paper we present the first reconstruction of organic material inputs from terrestrial sources, based on the analysis of long-chain n-alkanes and n-alkan-1-ols, in the subtropical western North Atlantic. $C_{23}-C_{33}$ odd carbon numbered n-alkanes and $C_{20}-C_{30}$ even carbon numbered n-alkan-1-ols are wax components of higher plant leaves [*Eglinton and Hamilton*, 1967] that allow the monitoring of continental inputs in recent [e.g., *Gagosian and Peltzer*, 1986] or ancient [e.g., *Poynter et al.*, 1989; *Prahl et al.*, 1994; *Villanueva et al.*, 1997a] open marine environments. Our study of the sedimentary record of higher plant n-alkanes and n-alkan-1-ols from the subtropical western North Atlantic Ocean reveals an abrupt variability in these continental inputs that is attributed to major changes in the atmospheric regime, with high increases in average wind strength during the cold episodes of the marine isotope stage 3 (D/O stadials).

2. Oceanographic and Climatic Setting

[4] The sediments analyzed were obtained from a spliced marine record based on three holes drilled at Site 1060, during the ODP Leg 172 [*Keigwin et al.*, 1998]. The studied ODP Site 1060 (30°46′N, 74°28′W, 3481 m water depth; Figure 1) is located at the Blake Outer Ridge, on the edge of the subtropical gyre, under the influence of the Gulf Stream [*Keigwin et al.*, 1998]. At present, the site is bathed by the

---

[1]Department of Environmental Chemistry, Instituto de Investigaciones Químicas y Ambientales de Barcelona, Consejo Superior de Investigaciones Científicas, Barcelona, Catalonia, Spain.

[2]Godwin Institute for Palaeoclimate Research, Department of Earth Sciences, University of Cambridge, Cambridge, UK.

[3]Fachbereich Geowissenschaften, Universität Bremen, Bremen, Germany.
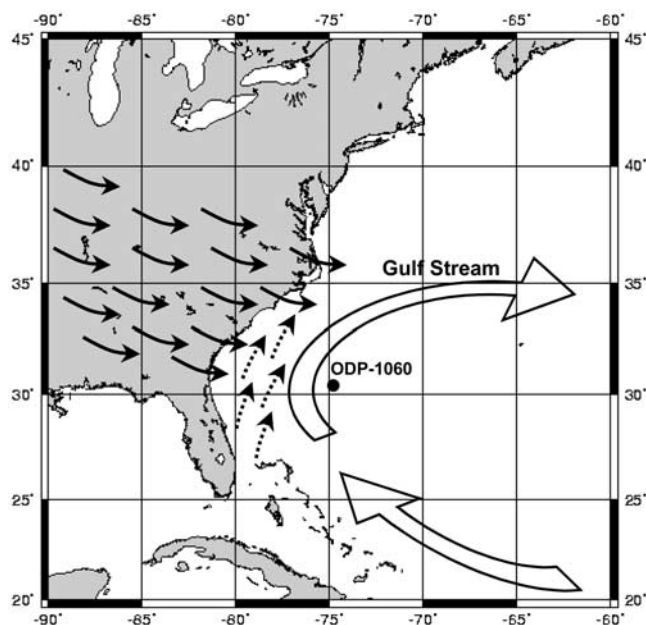
[4]Now at British Antarctic Survey, Cambridge, UK.

Figure 1. Map showing the location of core ODP Site 1060 in the Blake Outer Ridge. Open arrows indicate surface ocean circulation. Solid and dashed arrows indicate the present wind direction in winter and summer, respectively [*Bryson and Hare*, 1974].

North Atlantic Deep Water (NADW) carried by the Deep Western Boundary Current (DWBC) [*McCave and Tucholke*, 1986].

[5] The latitude of ODP Site 1060 (approximately. 31°N) lies under the influence of the westerlies. At present, maximum westerlies shift from the southeastern US in winter to southern Canada in summer. This movement is related to the summer expansion of the intertropical convergence zone involving the development of the North American monsoon system [*Yu and Wallace*, 2000] that is characterized by negative sea level pressure anomalies and high summer rains [*Adams and Comrie*, 1997]. During this season, winds blow along the coast following the Gulf Stream direction and, in winter, ODP Site 1060 is under the influence of the westerlies (Figure 1) [*Bryson and Hare*, 1974]. This latitudinal seasonal oscillation of the westerlies has been a common feature of the area throughout the Holocene [*Adams and Comrie*, 1997]. Vegetation studies suggest that glacial environmental conditions were dry and windy in the eastern and southeastern North America [*Watts*, 1979, 1980] corresponding to dominance of the westerlies during longer seasonal periods than in the Holocene.

3. Methods

3.1. Analysis of Sedimentary Lipids

[6] Sediment samples from core Site 1060 (0.5 cm thick slices) were taken every 4 cm. The analytical procedure for determining the organic biomarkers (*n*-alkanes, *n*-alkan-1-ols and C_{37}-alkenones) are described in detail by *Villanueva*

et al. [1997b]. Briefly, samples were freeze-dried and manually ground. After addition of an internal standard containing *n*-nonadecan-1-ol, *n*-hexatriacontane and *n*-tetracontane, *ca.* 2 g of dry sediment were extracted with dichloromethane in an ultrasonic bath. The extracts were saponified with 6% potassium hydroxide in methanol to eliminate interferences from wax esters. The neutral lipids were extracted with hexane which was then evaporated to dryness under a N_2 stream. Finally, the extracts were redissolved with toluene, derivatized with bis(trimethylsilyl) trifluoroacetamide and analyzed by gas chromatography.

[7] The instrumental analysis of the samples was performed with a Varian gas chromatograph model 3400 equipped with a septum-programmable injector (Varian 8200CX) and a flame ionization detector. The carrier gas (hydrogen, 2.6 mL/min) passed through a CPSIL-5 CB column coated with 100% dimethylsiloxane (50 m long, 0.12 μm film thickness). The temperature program of the oven was as follows: the initial temperature 90°C was maintained 1 min and then increased to 170°C at 20°C/min, then to 280°C at 6°C/min (holding time: 25 min) and, finally, to 315°C at 10°C/min (holding time: 12 min). The injector was programmed from 90°C (holding time 0.5 min) to 310°C at 200°C/min (holding time: 55 min). The detector was maintained with a constant temperature of 320°C.

[8] Selected samples were analyzed by gas chromatography coupled to mass spectrometry (GC-MS) for compound verification and identification of possible coelutions. GC-MS was performed with a Fisons MD800 (THERMO Instruments, Manchester, U.K.). The capillary column and the oven conditions were the same as described above. The carrier gas was He at a flow of 2.1 mL/min. Injection port and transfer line temperatures were 300°C. The quadrupole mass spectrometer was operated in EI mode (70 eV), scanning between m/z 50–650 in 1 s. The ion source temperature was 200°C.

[9] Concentrations (expressed as ng/g of dry weight sediment) were calculated using the internal standard (*n*-hexatriacontane). Fluxes (F; μg/cm^2/kyr) were calculated as follows: $F = C * DBD * SR$, where C is concentration (μg/g of dry sediment), DBD is dry bulk density (g/cm^3 of dry sediment) [*Keigwin et al.*, 1998] and SR is sedimentation rate (cm/kyr). Sea surface temperatures were based on the $U_{37}^{K'}$ index, which was calibrated to temperature with the equation ($U_{37}^{K'} = 0.033 * SST + 0.044$) [*Müller et al.*, 1998].

[10] Compound specific carbon isotope analyses of the aliphatic hydrocarbons were performed with a Agilent 6890 gas chromatograph coupled to a Delta Plus isotope ratio mass spectrometer using a GC-C combustion III (Thermo-Finnigan) interface. The instrument was equipped with a DB-5MS column (30 m long, 0.25 mm internal diameter, 0.25 μm film thickness) that was operated with the following temperature program: initial temperature 60°C maintained 1 min and then increased to 170°C at 12°C/min and to 280°C at 6°C/min and to 315°C at 10°C/min with a final holding time of 12 min. The temperature of the injector was 270°C. The CuO/NiO/Pt combustion reactor was set at 940°C. The reproducibility of the isotopic data was assessed by replicate analyses of laboratory standards (mix of deu-

terated *n*-alkanes in hexane) and ranged between 0.05 and 0.7‰.

3.2. Micropaleontological Analysis

[11] The method for taxonomy of planktonic foraminifera is described by *Vautravers et al.* [2004]. Data were obtained at the same resolution as the biomarkers allowing direct comparison between the two series of proxies. Prior to all analyses, 10 cm³ samples were disaggregated in distilled water, and wet sieved at 63 μm. The fraction smaller than 63 μm was retained by sediment settling and decantation and the fraction larger than 63 μm was dry sieved through a
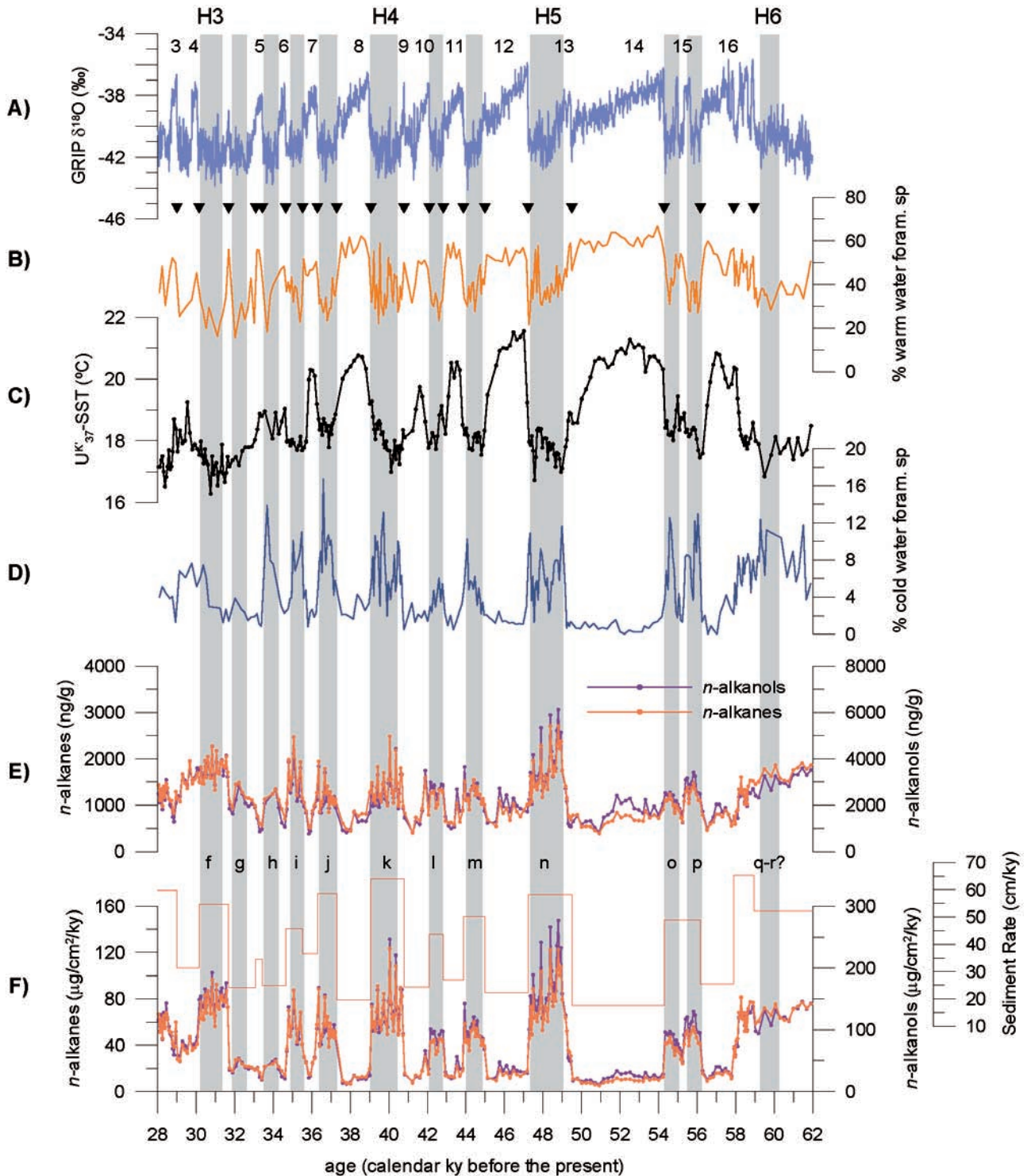

Figure 2

150 μm sieve. Where necessary this last fraction was divided using a micro splitter until about 350 to 500 planktonic foraminifera were obtained for micropaleontological study. Taxonomy of planktonic foraminifera was performed on the >150 μm fraction size using a gridded tray and following methods described in previous reports [*Parker*, 1962; *Be*, 1977]. Any samples containing fewer than 100 whole planktonic foraminifera specimens were not retained in the calculation because they were considered to fall below the statistical reliability threshold.

3.3. Carbonate Analysis

[12] Carbonate content (%CaCO$_3$) was derived from X-ray fluorescence (XRF) measurements performed with a non destructive core scanner at the University of Bremen. Ca element intensities (in counts/s) were measured with the core scanner at a 2-cm resolution on the archive halves of the cores. Ca intensities were converted to CaCO$_3$ concentrations (wt %) by applying a regression equation that was derived from a linear correlation (r = 0.94) of scanner measurements and 100 CaCO$_3$ analyses on discrete samples (using a LECO-Analyzer). Subsequently the resulting data set was averaged and resampled to match the resolution of the organic biomarker records.

3.4. Grain-Size Analysis

[13] The clay and silt fractions (<63 μm) separated for micropaleontological study [*Vautravers et al.*, 2004] were retained and the particle size distributions were determined using a Micromeritics Sedigraph 5000 ET analyzer. The procedure and the computer interface used in processing the raw data are described by *Jones et al.* [1988] and *Bianchi et al.* [1999].

3.5. Chronostratigraphy

[14] The development of the age model is explained in detail by *Vautravers et al.* [2004]. Because of the low concentration of foraminifera at this site, it is not practical to establish either a continuous planktonic δ^{18}O record or ^{14}C chronology. Instead, a timescale is constructed on the basis of the variations in the percentage of a group of warm surface-dwelling planktonic foraminifera. This "warm" group (Figure 2b) is mainly made up of specimens of the genus Globerinoides (*Globigerinoides ruber*, and *Globigerinoides sacculifer*), but also includes *Globigerinella aequilateralis*, *Orbulina universa*, *Globigerina falconensis*, *Globigerina digitata*, *Globigerina rubescens*, *Globigerinoides tenelus* and *Pulleniatina obliquiloculata*. This group of planktonic foraminifera was utilized instead of the cold species group *Neogloboquadrina pachyderma* and *Turbor-*

otalita quinqueloba because it only shows minor and generally smooth fluctuations (Figure 2d). Age control points were set on the same basis as for core MD95-2042 off Portugal [*Shackleton et al.*, 2000] linking the sudden changes in surface water to changes in Greenland atmospheric temperature estimated from the ice δ^{18}O on the SSO9 sea timescale for the GRIP core [*Johnsen et al.*, 2001] following the modifications of *Shackleton et al.* [2004] for the age of the ice core (Figure 2a). The pattern of fluctuations in the "warm" group of species convincingly resembles the Greenland temperature record. Thus 23 age control points between 22.6 and 64.82 ka were inserted by reference to these transitions on the SSO9 sea timescale [see *Vautravers et al.*, 2004, Table 1] (the 21 age control points included in the period studied in the present work are shown in Figure 2b). The resulting sedimentation rates (Figure 2f) range between 20 cm and 70 cm/kyr, with the highest values systematically found during stadials. Sampling and analysis provided a mean time resolution of 120 $\pm$ 68 years.

[15] The construction of the age model using planktonic foraminifera minimizes the problems of erecting a stratigraphy in sediment drifts as described from Bermuda Rise sites [*Ohkouchi et al.*, 2002; *McCave*, 2002] since planktonic shells that are larger than 150 mm sink quickly to the bottom. Thus the age scale developed for Site 1060 should not be significantly affected by potential problems related to the mobility of the fine organic matter fraction [*Ohkouchi et al.*, 2002] although it should be noted that this problem has not been identified on the BOR. Our faunal-based age model is consistent with the age model developed by *Hagen and Keigwin* [2002] for the nearby and shallower Site 1059, where enough material for AMS ^{14}C dating on planktonic foraminifera was available.

4. Results

4.1. Inputs of Higher Plant Compounds at the Blake Outer Ridge

[16] The concentrations and fluxes of higher plant *n*-alkanes and *n*-alkan-1-ols at Site 1060 exhibit an abrupt pattern following the D/O climate variability (Figure 2e and 2f). Increases of these terrigenous compounds coincide with cold events, marked by U$^{K'}_{37}$-SST minima (Figure 2c) and cold water foraminifera species maxima (Figure 2d and Table 1). The flux changes between Greenland interstadials and stadials (GISs and GSs, respectively) involve variations from 5.4 to 120 μg/cm^2/kyr and 11 to 280 μg/cm^2/kyr for the *n*-alkanes and *n*-alkan-1-ols, respectively (Figure 2f). Concentration or flux increases of four and three times for the *n*-alkan-1-ols and the *n*-alkanes, respectively, occur in

Figure 2. (a) Atmospheric δ^{18}O in GRIP [*Johnsen et al.*, 2001] on the timescale of *Shackleton et al.* [2004]. Heinrich events are indicated on top (H); isotopically defined Greenland interstadials (GIS) are also indicated. (b) Percent of warm water surface foraminifera species (*G. ruber*, *G. sacculifer*, *G. aequilateralis*, *O. universa*, *G. falconensis*, *G. digitata*, *G. rubescens*, *G. tenelus*, and *P. obliquiloculata*) used for the age model of ODP-1060 [*Vautravers et al.*, 2004]. Age control points are also indicated. (c) U$^{K'}_{37}$ sea surface temperature in ODP-1060. (d) Percent of cold water surface foraminifera species (*T. quinqueloba* and *N. pachyderma*) in ODP-1060 [*Vautravers et al.*, 2004]. (e) Concentrations of C$_{23}$−C$_{33}$ *n*-alkanes and C$_{20}$−C$_{30}$ *n*-alkan-1-ols. They record higher plant continental inputs to ODP-1060. (f) Fluxes of C$_{23}$−C$_{33}$ *n*-alkanes and C$_{20}$−C$_{30}$ *n*-alkan-1-ols in ODP-1060. They are labeled following *Rohling et al.* [2003]; sediment rate is also shown. Shaded areas indicate cold events (Heinrich events and Greenland stadials).

Table 1. Average Values of *n*-Alkane and *n*-Alkan-1-ol Fluxes and Concentrations in Core Ocean Drilling Program Site 1060 for the Greenland Stadials and Interstadials[a]

GRIP Events	N	Fluxes		Concentrations	
		n-Alkanes	*n*-Alkan-1-ols	*n*-Alkanes	*n*-Alkan-1-ols
GIS-16	9	14 ± 3	31 ± 7	700 ± 140	1600 ± 380
GS-16	9	48 ± 6	110 ± 15	1300 ± 150	2800 ± 400
GIS-15	2	26 ± 2	56 ± 13	680 ± 60	1500 ± 330
GS-15	6	42 ± 3	94 ± 2	1120 ± 80	2500 ± 60
GIS-14	22	9 ± 2	23 ± 6	690 ± 140	1700 ± 430
GS-13	25	80 ± 20	172 ± 48	1800 ± 450	3800 ± 1050
GIS-12	11	15 ± 3	33 ± 8	850 ± 170	1900 ± 450
GS-12	13	48 ± 7	102 ± 17	1240 ± 190	2600 ± 440
GIS-11	4	13 ± 1	25 ± 5	620 ± 30	1200 ± 220
GS-11	8	41 ± 5	92 ± 8	1220 ± 150	2700 ± 250
GIS-10	5	13 ± 4	25 ± 6	720 ± 200	1300 ± 340
GS-9	26	70 ± 18	132 ± 37	1400 ± 370	2700 ± 740
GIS-8	8	12 ± 4	19 ± 5	760 ± 260	1250 ± 330
GS-8	15	56 ± 14	103 ± 26	1230 ± 310	2300 ± 570
GIS-7	2	15 ± 1	24 ± 2	520 ± 20	830 ± 80
GS-7	8	58 ± 16	106 ± 29	1650 ± 450	3000 ± 810
GIS-6	2	16 ± 3	22 ± 2	810 ± 150	1150 ± 110
GS-6	3	24 ± 2	47 ± 6	1240 ± 110	2400 ± 310
GIS-5	12	21 ± 5	37 ± 10	1100 ± 300	1900 ± 570
GS-5	20	75 ± 11	152 ± 16	1800 ± 260	3600 ± 390

[a]Flux values are given in $\mu g/cm^2/kyr$; concentrations are given in ng/g. Flux and concentration averages plus/minus standard deviation are given. Abbreviations are GRIP, Greenland Ice Core Project; GS, Greenland stadials; GIS, Greenland interstadials; and N, number of samples.

less than 400 years, such as at the beginning of GS-13 which coincides with the Heinrich Event 5 (HE5) (Figure 2f). At the start of GS-8 (onset of HE4), *n*-alkan-1-ols fluxes increased six times and those of *n*-alkanes over five times within 150 years (Figure 2f).

[17] The occurrence of these biomarkers in marine sediments located far away from the influence of coastal discharges is generally attributed to inputs carried by wind [*Gagosian and Peltzer*, 1986; *Gagosian et al.*, 1987; *Huang et al.*, 2000]. Aerosol studies at nearby sites (e.g., Bermuda) indicate that leaf wax biomarkers are effectively air transported from North America into the open North Atlantic [*Conte and Weber*, 2002b]. The *n*-alkane and *n*-alkan-1-ol homologues at Site 1060 are maximized at $C_{29}-C_{31}$ and C_{28}, respectively (Figure 3), as observed in the aerosols carried by the westerlies into the Atlantic Ocean [*Conte and Weber*, 2002a]. However, possible contributions from non-eolian processes in ODP-1060 site should also be considered. They will be evaluated below.

4.1.1. Fluvial Discharges

[18] Site 1060 is located more than 500 km from the present coastline and at 3481 m water depth. Sea level was 60–90 m below the present level during marine isotope stage 3 (MIS3) [*Lea et al.*, 2002; *Waelbroeck et al.*, 2002; *Cutler et al.*, 2003], while at the Last Glacial Maximum (LGM) sea level was about 120 m below the present height [*Fairbanks*, 1989]. Given the shape of the continental platform in eastern North America, this could involve a seaward extension of the present coastline of about 14 km at the most. It therefore seems unlikely that fluvial discharges would have been the cause of significant sediment transport to the study site either in stadial or interstadial periods [*Giosan et al.*, 2002]. This assumption is in agreement with

models of freshwater runoff that show that during GSs drainage of North America into the North Atlantic occurred via the Mississippi River system [*Marshall and Clarke*, 1999]. It is also in agreement with the increase in flux of sedimentary materials from eastern Canada in the glacial periods [*Keigwin and Jones*, 1994; *Giosan et al.*, 2002], namely, in GSs [*Keigwin and Jones*, 1994].

[19] In the absence of nearby strong river plumes (as in Mississippi or Hudson rivers), little terrigenous organic material could be expected to be carried 500 km offshore in surface water since in general the great majority of continental organic matter dissolved or suspended in particles from freshwater flows tend to aggregate and settle to the seabed upon discharge into the sea [*Grimalt and Albaiges*, 1990; *Takada et al.*, 1994; *Tolosa et al.*, 1996].

4.1.2. Ice-Rafted Debris

[20] The sediment sections of Site 1060 exhibit very low contents of ice-rafted debris (IRD > 90 μm). Comparison of the terrigenous biomarkers and IRD exhibits some rough degree of concurrence in a few episodes as both proxies show, in general, increasing concentrations in the GSs (Figures 4b, 4f, and 4g). However, close examination of both proxies shows that the concordance is very weak since there is no parallelism in the relative intensities of IRD and higher plant markers and there is no agreement in the age interval of the GS episodes of these two records (Figures 4b, 4f, and 4g). The higher amounts of the lithic counts, namely, those coinciding with (HE), are consistent with the IRD inputs in the North Atlantic during these episodes [*Vautravers et al.*, 2004]. IRD may contain *n*-alkanes but they exhibit distributions without odd carbon number preferences as it is characteristic of higher plants [*Martrat et al.*, 2003; *Villanueva et al.*, 1997a]. Furthermore, these materials do
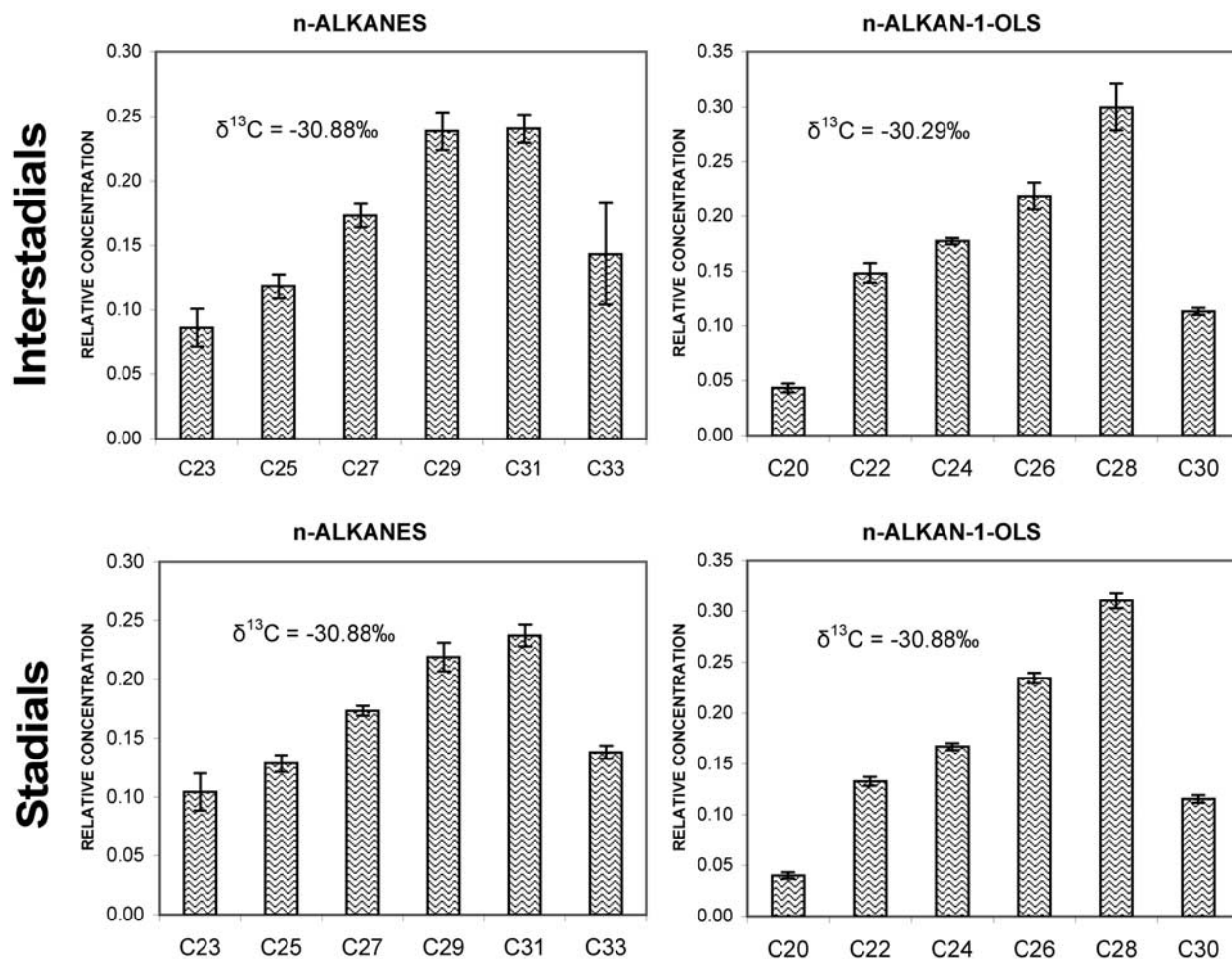
Figure 3. Average distributions of the higher plant n-alkanes and n-alkan-1-ols in the sections of core ODP-1060 corresponding to the Greenland stadials and interstadials. Error bars indicate standard deviation. The weighted mean of the $\delta^{13}C$ values of the n-alkane and n-alkan-1-ol homologues in these average distributions are also indicated.

not contain higher plant n-alkan-1-ols [*Martrat et al.*, 2003]. Therefore the higher plant biomarkers observed at Site ODP1060 cannot therefore be attributed to IRD inputs.

4.1.3. Lateral Advection and Resuspension

[21] Lateral advection by deep currents that can erode fine-grained material from continental margins should also be considered among the potential sources of the terrigenous biomarkers. Radiocarbon age discrepancies between the fine organic matter (<63 um), including the algal C_{37} alkenones, and coexisting foraminifera, arguably due to lateral transport and resuspension, have been described in sediments from the Bermuda Rise [*Ohkouchi et al.*, 2002]. The higher plant n-alkan-1-ols and n-alkanes of Site 1060 do not appear to undergo these effects, as changes in their concentrations show a strong correlation ($0.594 < r < 0.817$, $n = 286$) with the variability of the faunal proxies (percentage of warm and cold surface water foraminifera species >150 μm, Figure 2) that belong to the coarse particle fraction (>63 μm).

Figure 4. (a) Atmospheric $\delta^{18}O$ in GRIP [*Johnsen et al.*, 2001] in the timescale of *Shackleton et al.* [2004]. Heinrich events are indicated on top (H); isotopically defined Greenland interstadials (GIS) are also indicated. (b) Ice-rafted detritus (concentration of quartz grains in the $90-150$ μm fraction) in ODP-1060 [*Vautravers et al.*, 2004]. (c) Sand flux (fraction >63 μm) in ODP-1060. (d) Silt/clay ratio (fraction <63 μm) in ODP-1060. (e) Concentrations of total C_{37} alkenones. They record algal inputs (hapthophyte algae) to ODP-1060. (f) Concentrations of $C_{23}-C_{33}$ n-alkanes and $C_{20}-C_{30}$ n-alkan-1-ols. They record higher plant continental inputs to ODP-1060. (g) Fluxes of $C_{23}-C_{33}$ n-alkanes and $C_{20}-C_{30}$ n-alkan-1-ols in ODP-1060. They are labeled following *Rohling et al.* [2003]. (h) Polar Circulation Index (PCI) in GISP2 [*Mayewski et al.*, 1997] and Ca^{2+} in GRIP. Shaded areas indicate cold events (Heinrich events and Greenland stadials).
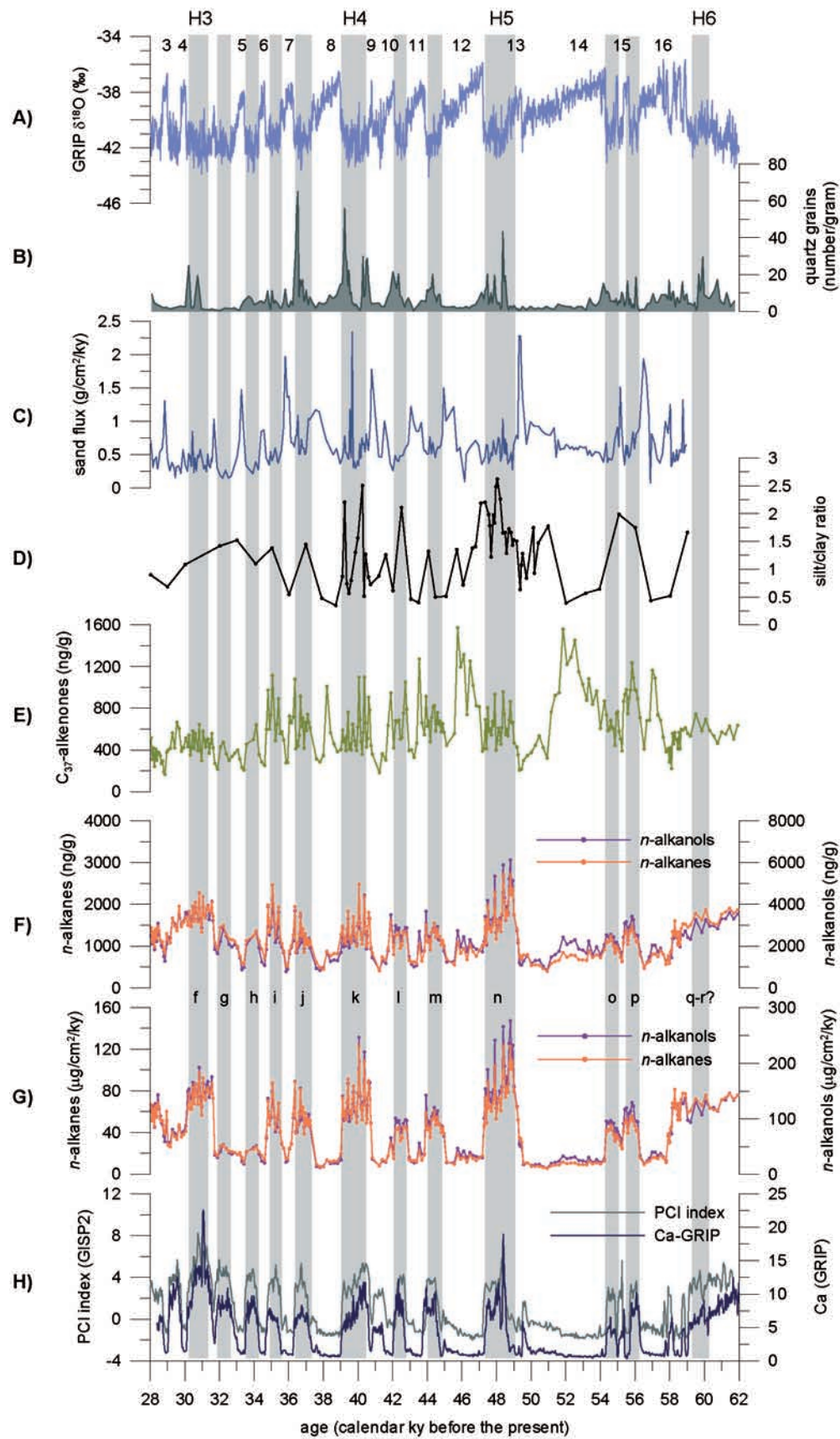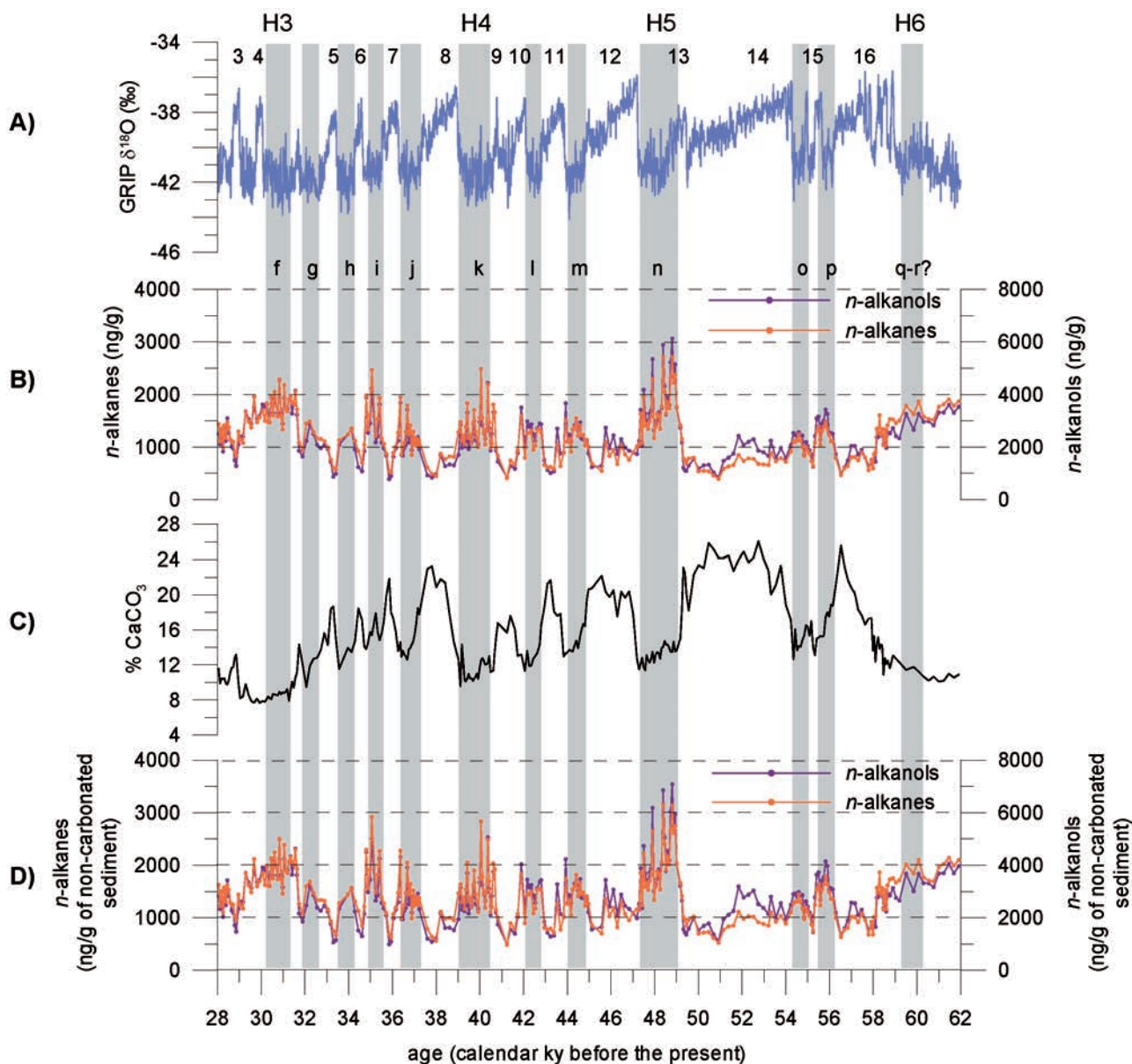
Figure 4

Figure 5. (a) Atmospheric $\delta^{18}O$ in GRIP [*Johnsen et al.*, 2001] in the timescale of *Shackleton et al.* [2004]. Heinrich events are indicated on top (H); isotopically defined Greenland interstadials (GIS) are also indicated. (b) Concentrations of $C_{23}-C_{33}$ *n*-alkanes and $C_{20}-C_{30}$ *n*-alkan-1-ols. (c) Percentage of calcium carbonate in Site 1060. (d) Concentrations of $C_{23}-C_{33}$ *n*-alkanes and $C_{20}-C_{30}$ *n*-alkan-1-ols referred to the noncarbonated sediment.

4.2. Marine Productivity

[22] Carbonate content is an important aspect in relation to marine productivity. The changes in carbonate concentration at ODP Site 1060 core exhibit a D/O pattern involving higher values during GISs (Figure 5). These concentrations and MIS3 climate variability are in agreement with previous reports from nearby cores [e.g., *Keigwin and Jones*, 1994]. However, normalization of the concentrations of both *n*-alkanes and *n*-alkan-1-ols to the noncarbonate sedimentary fraction does not change the previously reported differences between GSs and GISs

(Figure 5). Thus, the concentration changes of terrigenous lipids between these two MIS3 stages are not due to dilution effects following the variations in carbonate content.

4.3. Origin of the Vegetation Source

[23] The stable carbon isotope composition of these higher plant biomarkers measured by weighted average of the $\delta^{13}C$ values of the constituent homologues [*Zhang et al.*, 2003] shows a remarkable uniformity between GSs and GISs. In the *n*-alkan-1-ols these mean values are −30.88‰ and −30.29‰, respectively, and in the *n*-alkanes −30.88‰ in both cases (Table 2 and Figure 3). The $\delta^{13}C$ measure-

Table 2. Weighted Average Values of $\delta^{13}C$ in *n*-Alkanes and *n*-Alkan-1-ols for the Greenland Stadials and Interstadials of Core ODP-1060[a]

GRIP Events	*n*-Alkan-1-ols ($C_{20}-C_{28}$), ‰	*n*-Alkanes ($C_{23}-C_{31}$), ‰
GS-8	−31.23 (−30.84, −32.13)	−30.99 (−30.41, −31.68)
GIS-8	−30.92 (−29.45, −32.05)	−31.66 (−31.32, −31.97)
GS-9	−32.15 (−30.17, −33.34)	−30.56 (−29.74, −31.51)
GS-11	−30.53 (−30.03, −30.84)	−31.24 (−30.26, −31.86)
GIS-11	−29.75 (−27.91, −30.59)	−30.43 (−28.93, −30.92)
GS-12	−30.53 (−29.47, −31.24)	−30.58 (−29.35, −31.37)
GIS-12	−29.49 (−27.65, −30.45)	−30.24 (−29.08, −31.14)
GS-13	−29.98 (−29.18, −30.34)	−31.02 (−29.67, −32.89)
GIS-16	−31.01 (−29.42, −31.94)	−31.20 (−30.07, −31.76)

[a]Average values are calculated as described by *Zhang et al.* [2003]. Interval of values is indicated within parentheses.

ments of the alcohols are in strong agreement with those determined at present in aerosols from North American air masses collected at Bermuda [*Conte and Weber*, 2002b] and both *n*-alkane and *n*-alkan-1-ol values correspond to dominant inputs from C_3 plants [*Huang et al.*, 2000, 2001]. The strong similarity of the average composition in GSs and GISs indicates that the vegetation sources of the higher plant inputs recorded at Site 1060 did not change significantly during either type of periods. This lack of change is also supported by the strong similarity in the distributions of higher plant *n*-alkanes and *n*-alkan-1-ols in the GSs and GISs (Figure 3). Thus, the higher amounts of these terrigenous proxies in the GSs do not reflect changes in source origin.

4.4. Deep Water Ventilation During GSs and GISs

[24] Records derived from the lithogenic fraction indicate that there is no significant correlation between terrigenous biomarkers and sand (>63 μm, mainly foraminifera) or mud (<63 μm) fluxes. Patchy correspondences between alkenone, *n*-alkane and *n*-alkan-1-ol concentrations and fluxes and silt/clay (S/C) ratios are apparent (Figure 4). The silt/clay ratio is high (i.e., low proportion of clay) at several times of high concentration and flux of terrigenous biomarkers. There are also some times when the relationship is opposite, e.g., 50–52 kyr B.P., which explains the poor correlation coefficient (r = 0.42) for the whole series. The times of low clay% (high S/C ratio) were quite often those of increased supply of higher plant alkanes and alkan-1-ols which in turn supports the view that these biomarkers were not carried by deep currents, or indeed by clays, but that they are independently supplied from the land, most likely by eolian transport.

[25] Furthermore, the D/O pattern of these concentration changes in Site 1060 is only found in the higher plant lipids and not in other biomarkers such as the marine algal C_{37} alkenones (Figure 4e). The concentrations of these alkenones are characteristic of oligotrophic waters [*Villanueva et al.*, 1998, 2001]. Because both C_{37} alkenones and higher plant *n*-alkanes and *n*-alkan-1-ols belong to a group of biomarkers that are most resistant to diagenesis [*Hoefs et al.*, 2002] dominant postdepositional transformation processes would have led to distributions of both biomarker

groups paralleling the D/O differences. The absence of a common D/O pattern in the concentrations of these biomarkers of different origins also argues against accumulation processes related to lateral advection for the increments in higher plant lipids during GSs.

[26] The *n*-alkanols are more susceptible to degradation than *n*-alkanes [*Hoefs et al.*, 2002]. Postdepositional oxidation of sedimentary lipids by changes in bottom redox conditions should therefore be reflected in preferential depletion of *n*-alkan-1-ol concentrations with respect to those of the *n*-alkanes. This selective depletion has been observed, for instance, in the Alboran Sea where higher ventilation due to increases of deep currents resulted in decreases of the relative content of higher plant *n*-alkan-1-ols versus *n*-alkanes [*Cacho et al.*, 2000]. At Site 1060, both higher plant biomarkers exhibit parallel records throughout the whole studied period (r = 0.942) (Figure 2) which excludes changes in deep water ventilation during the GSs [*Hagen and Keigwin*, 2002] as a significant process for modification of their concentration.

5. Discussion: Higher Plant *n*-Alkanes and *n*-Alkan-1-ols as Wind Markers in the Subtropical Western North Atlantic

[27] The sedimentary fluxes of higher plant *n*-alkanes and *n*-alkan-1-ols found in this study (average values of 9–80 $\mu g/cm^2/kyr$ and 19–170 $\mu g/cm^2/kyr$, respectively; Table 1) are similar or lower than the atmospheric deposition fluxes of these compounds found at present in open marine systems. Thus, extrapolation of the fluxes of higher plant *n*-alkanes and *n*-alkan-1-ols measured in the central equatorial north Pacific [*Gagosian and Peltzer*, 1986] shows values of 33 and 19 $\mu g/cm^2/kyr$, respectively. Extrapolation of the higher plant *n*-alkane atmospheric deposition fluxes in the open western Mediterranean [*Grimalt et al.*, 1988] gives values of 40–440 $\mu g/cm^2/kyr$. Accordingly, comparison of atmospheric and sedimentary fluxes of these higher plant biomarkers in remote open marine sites shows that the former may have a major potential impact on the inventory of terrestrially derived lipid material found in deep-sea organic carbon [*Gagosian and Peltzer*, 1986].

[28] Atmospheric teleconnections have been invoked to explain the nearly synchronous changes between $\delta^{18}O$ in Greenland ice and marine sedimentary records at middle-low latitudes of the Northern Hemisphere during MIS3 [*Cacho et al.*, 1999; *Peterson et al.*, 2000]. In the subtropical western North Atlantic, the abrupt climatic changes in $U^{K'}_{37}$-SST paralleling those in Greenland have also been explained assuming common atmospheric interactions [*Vautravers et al.*, 2004]. The profiles of air transported higher plant biomarkers at Site 1060 (Figures 4f and 4g) provide direct evidence of this atmospheric teleconnection, showing higher wind intensities in GSs than in GISs. Studies on lithogenic fraction and pollen records in the eastern North Atlantic have also shown rapid climate changes related with rapid reorganizations of the atmospheric circulation, suggesting an enhancement of the wind

system (the north westerlies) during GSs [*Moreno et al.*, 2002, 2005; *Sanchez-Goñi et al.*, 2002].

[29] The flux records of *n*-alkanes and *n*-alkan-1-ols from ODP Site 1060 (Figures 4g and 4h) show a very good match with the changes in Ca^{2+} of GRIP or the polar circulation index (PCI) in GISP2 [*Mayewski et al.*, 1997] (calculated from cations representing the records of atmospheric dust and sea salt ions, e.g., K^+, Ca^{2+} and Mg^{2+}), indicates a very good match with the flux records of *n*-alkanes and *n*-alkan-1-ols from ODP-1060 core (Figures 4g and 4h). According to this agreement, the strong increases in biomarkers reflecting wind strength during the GSs at 31°N represent a general phenomenon of the Northern Hemisphere that was related to a significant reinforcement of the westerlies. Studies on mineral dust in NGRIP Greenland ice core [*Ruth et al.*, 2003] and Chinese Loess during MIS3 [e.g., *Porter and An*, 1995] are also consistent with increasing wind activity during GSs.

[30] The fluxes of these higher plant biomarkers can be used for the evaluation of the changes in wind strength during MIS3. For comparison, every peak in the flux record has been labeled as was done in a previous study of cations from continental sources in GISP2 [*Rohling et al.*, 2003] (Figure 4g). At Site 1060, the concentrations and fluxes associated with the GSs are much higher when coinciding with the Heinrich events (HEs) (Figure 4), even in the case of HE3. This event is characterized neither by high IRD amounts nor by a well defined abrupt SST drop. However, the strong increase of higher plant biomarkers during HE3 is consistent with the observed increases of PCI and Ca^{2+} content in the Greenland cores. The concurrence of these atmospheric markers despite the lower signal of HE at Site 1060 strengthens the argument of both air proxies as indicators of the general increase of wind speed in the Northern Hemisphere during the GSs. In these periods, the likely southward shift of the Intertropical Convergence Zone and the associated trade wind belt [*Peterson et al.*, 2000; *Vellinga and Wood*, 2002] led to increases of the westerlies.

6. Conclusions

[31] The concentration and fluxes of higher plant *n*-alkanes and *n*-alkan-1-ols in sediments of the Blake Outer Ridge record the significance of the eolian inputs of continental organic material arriving at this site. Their millennial-scale variability reveals an enhancement of the westerlies in the subtropical North Atlantic during the GSs. Comparison of these terrestrial biomarkers with other wind-related proxies from Greenland ice cores shows that the strengthening of the wind system was a general phenomenon of the Northern Hemisphere during the GSs.

[32] These abrupt changes in the wind regime paralleling the abrupt transitions from GIS to GS reflect increases of the intensities of the westerlies associated with slow down episodes of the overturning circulation. Calculations with a coupled ocean-atmosphere model with sea ice and land surface schemes to study the effects of collapses of the thermohaline circulation [*Vellinga and Wood*, 2002] also predict increased westerlies in the North Atlantic in these conditions. These results are in agreement with our observations from Site 1060.

References

Adams, D. K., and A. C. Comrie (1997), The North American monsoon, *Bull. Am. Meteorol. Soc.*, 78, 2197–2213.

Allen, J. R. M., et al. (1999), Rapid environmental changes in southern Europe during the last glacial period, *Nature*, 400, 740–743.

Be, A. W. H. (1977), A taxonomic and zoogeographic review of Recent planktonic foraminifera, in *Oceanic Micropaleontology*, edited by A. T. S. Ramsay, pp. 1–100, Elsevier, New York.

Bianchi, G. G., I. R. Hall, I. N. McCave, and L. Joseph (1999), Measurement of the sortable silt current speed proxy using the Sedigraph 5100 and Coulter Multisizer IIe: Precision and accuracy, *Sedimentology*, 46, 1001–1014.

Bond, G. C., W. S. Broecker, S. Johnsen, J. F. McManus, L. D. Labeyrie, J. Jouzel, and G. Bonani (1993), Correlations between climate records from North Atlantic sediments and Greenland ice, *Nature*, 365, 143–147.

Broecker, W. S. (1997), Thermohaline circulation, the Achilles heel of our climate system: Will man-made CO_2 upset the current balance?, *Science*, 278, 1582–1588.

Bryson, R. A., and F. K. Hare (1974), The climates of North America, in *Climates of North America*, edited by R. A. Bryson and F. K. Hare, pp. 1–47, Elsevier, New York.

Cacho, I., J. O. Grimalt, C. Pelejero, M. Canals, F. J. Sierro, J. A. Flores, and N. Shackleton (1999), Dansgaard-Oeschger and Heinrich event imprints in Alboran Sea paleotemperatures, *Paleoceanography*, 14, 698–705.

Cacho, I., J. O. Grimalt, F. J. Sierro, N. J. Shackleton, and M. Canals (2000), Evidence for enhanced Mediterranean thermohaline circulation during rapid climatic coolings, *Earth Planet. Sci. Lett.*, 183, 417–429.

Conte, M. H., and J. C. Weber (2002a), Long-range atmospheric transport of terrestrial biomarkers to the western North Atlantic, *Global Biogeochem. Cycles*, 16(4), 1142, doi:10.1029/2002GB001922.

Conte, M. H., and J. C. Weber (2002b), Plant biomarkers in aerosols record isotopic discrimination of terrestrial photosynthesis, *Nature*, 417, 639–641.

Cutler, K. B., R. L. Edwards, F. W. Taylor, H. Cheng, J. Adkins, C. D. Gallup, P. M. Cutler, G. S. Burr, and A. L. Bloom (2003), Rapid sea-level fall and deep-ocean temperature change since the last interglacial period, *Earth Planet. Sci. Lett.*, 206, 253–271.

Dansgaard, W., et al. (1993), Evidence for general instability of past climate from a 250-kyr ice-core record, *Nature*, 364, 218–220.

Eglinton, G., and R. J. Hamilton (1967), Leaf epicuticular waxes, *Science*, 156, 1322–1335.

Fairbanks, R. G. (1989), A 17,000-year glacio-eustatic sea level record: Influence of glacial melting rates on the Younger Dryas event and deep-ocean circulation, *Nature*, 342, 637–642.

Gagosian, R. B., and E. T. Peltzer (1986), The importance of atmospheric input of terrestrial organic material to deep sea sediments, *Org. Geochem.*, 10, 661–669.

Gagosian, R. B., E. T. Peltzer, and J. T. Merrill (1987), Long-range transport of terrestrially derived lipids in aerosols from the south Pacific, *Nature*, 325, 800–803.

Ganopolski, A., and S. Rahmstorf (2001), Rapid changes of glacial climate simulated in a coupled climate model, *Nature*, *409*, 153–158.

Giosan, L., R. D. Flood, and R. C. Aller (2002), Paleoceanographic significance of sediment color on western North Atlantic drifts: I. Origin of color, *Mar. Geol.*, *189*, 25–41.

Grimalt, J. O., and J. Albaiges (1990), Characterization of the depositional environments of the Ebro Delta (western Mediterranean) by the study of sedimentary lipid markers, *Mar. Geol.*, *95*, 207–224.

Grimalt, J. O., J. Albaiges, M. A. Sicre, J. C. Marty, and A. Saliot (1988), Aerosol transport of polynuclear aromatic hydrocarbons over the Mediterranean Sea, *Naturwissenschaften*, *75*, 39–42.

Hagen, S., and L. D. Keigwin (2002), Sea-surface temperature variability and deep water reorganisation in the subtropical North Atlantic during isotope stage 2–4, *Mar. Geol.*, *189*, 145–162.

Heinrich, H. (1988), Origin and consequences of cyclic ice rafting in the N-E Atlantic Ocean during the past 130,000 years, *Quat. Res.*, *29*, 142–152.

Hoefs, M. J. L., W. I. C. Rijpstra, and J. S. Sinninghe Damsté (2002), The influence of oxic degradation on the sedimentary biomarker record I: Evidence from Madeira Abyssal Plain turbidites, *Geochim. Cosmochim. Acta*, *66*, 2719–2735.

Huang, Y., L. Dupont, M. Sarnthein, J. M. Hayes, and G. Eglinton (2000), Mapping of C4 plant input from north west Africa into north east Atlantic sediments, *Geochim. Cosmochim. Acta*, *64*, 3505–3513.

Huang, Y., F. A. Street-Perrott, S. E. Metcalfe, M. Brenner, M. Moreland, and K. H. Freeman (2001), Climate change as the dominant control on glacial-interglacial variations in C3 and C4 plant abundance, *Science*, *293*, 1647–1651.

Johnsen, S. J., D. Dahl-Jensen, N. Gundestrup, J. P. Steffensen, H. B. Clausen, H. Miller, V. Masson-Delmotte, A. E. Sveinbjörnsdottir, and J. White (2001), Oxygen isotope and palaeotemperature records from six Greenland ice-core stations: Camp Century, Dye-3, GRIP, GISP2, Renland and NorthGRIP, *J. Quat. Sci.*, *16*, 299–307.

Jones, K. P. N., I. N. McCave, and P. D. Patel (1988), A computer-interfaced sedigraph for modal size analysis of fine-grained sediment, *Sedimentology*, *35*, 163–172.

Keigwin, L. D., and E. A. Boyle (1999), Surface and deep ocean variability in the northern Sargasso Sea during marine isotope stage 3, *Paleoceanography*, *14*, 164–170.

Keigwin, L. D., and G. A. Jones (1994), Western North Atlantic evidence for millennial-scale changes in ocean circulation and climate, *J. Geophys. Res.*, *99*, 12,397–12,410.

Keigwin, L. D., D. Rio, and G. D. Acton (1998), *Proceedings of the Ocean Drilling Program Initial Reports*, Ocean Drill. Program, College Station, Tex.

Lea, D. W., P. A. Martin, D. K. Pak, and H. J. Spero (2002), Reconstructing a 350 ky history of sea level using planktonic Mg/Ca and oxygen isotope records from a Cocos Ridge core, *Quat. Sci. Rev.*, *21*, 283–293.

Leuschner, D. C., and F. Sirocko (2000), The low-latitude monsoon climate during Dansgaard-Oeschger cycles and Heinrich events, *Quat. Sci. Rev.*, *19*, 243–254.

Marshall, S. J., and G. K. C. Clarke (1999), Modeling North American freshwater runoff through the last glacial cycle, *Quat. Res.*, *52*, 300–315.

Martrat, B., J. O. Grimalt, J. Villanueva, S. van Kreveld, and M. Sarnthein (2003), Climatic dependence of the organic matter contributions in the north eastern Norwegian Sea over the last 15,000 years, *Org. Geochem.*, *34*, 1057–1070.

Mayewski, P. A., L. D. Meeker, M. S. Twickler, S. Whitlow, Q. Yang, W. B. Lyons, and M. Prentice (1997), Major features and forcing of high-latitude Northern Hemisphere atmospheric circulation using a 110,000-year-long glaciochemical series, *J. Geophys. Res.*, *102*, 26,345–26,366.

McCave, I. N. (2002), A poisoned chalice?, *Science*, *298*, 1186–1187.

McCave, I. N., and B. E. Tucholke (1986), Deep current-controlled sedimentation in the western North Atlantic, in *The Geology of North America*, edited by P. R. Vogt and B. E. Tucholke, pp. 541–468, Geol. Soc. of Am., Boulder, Colo.

McManus, J. F., D. W. Oppo, and J. L. Cullen (1999), A 0.5-million-year record of millennial-scale climate variability in the North Atlantic, *Science*, *283*, 971–975.

Moreno, A., I. Cacho, M. Canals, M. A. Prins, M. F. Sanchez-Goñi, J. O. Grimalt, and G. J. Weltje (2002), Saharan dust transport and high-latitude glacial climatic variability: The Alboran Sea record, *Quat. Res.*, *58*, 318–328.

Moreno, A., I. Cacho, M. Canals, J. O. Grimalt, M. F. Sanchez-Goñi, N. Shackleton, and F. Sierro (2005), Links between marine and atmospheric processes oscillating on a millennial time-scale: A multi-proxy of the last 50,000 yr from the Alboran Sea (western Mediterranean Sea), *Quat. Sci. Rev.*, *24*, 1623–1636.

Müller, P. J., G. Kirst, G. Ruhland, I. von Storch, and A. Rosell-Melé (1998), Calibration of the alkenone paleotemperature index UK'37 based on core-tops from the eastern South Atlantic and the global ocean (60°N–60°S), *Geochim. Cosmochim. Acta*, *62*, 1757–1772.

Ohkouchi, N., T. I. Eglinton, L. D. Keigwin, and J. M. Hayes (2002), Spatial and temporal offsets between proxy records in a sediment drift, *Science*, *298*, 1224–1227.

Parker, F. L. (1962), Planktonic foraminiferal species in Pacific sediments, *Micropaleontology*, *8*, 219–254.

Peterson, L. C., G. H. Haug, K. A. Hughen, and U. Röhl (2000), Rapid changes in the hydrologic cycle of the tropical Atlantic during the last glacial, *Science*, *290*, 1947–1951.

Porter, S. C., and Z. An (1995), Correlation between climate events in the North Atlantic and China during the last glaciation, *Nature*, *375*, 305–308.

Poynter, J. G., P. Farrimond, N. Robinson, and G. Eglinton (1989), Aeolian-derived higher plant lipids in the marine sedimentary record: Links with palaeoclimate, in *Paleoclimatology and Paleometeorology: Modern And Past Patterns of Global Atmospheric Transport*, edited by M. Leinen and M. Sarnthein, pp. 435–462, Springer, New York.

Prahl, F. G., J. R. Ertel, M. A. Goni, M. A. Sparrow, and B. Eversmeyer (1994), Terrestrial organic carbon contributions to sediments on the Washington margin, *Geochim. Cosmochim. Acta*, *58*, 3035–3048.

Rohling, E. J., P. A. Mayewski, and P. Challenor (2003), On the timing and mechanism of millennial-scale climate variability during the last glacial cycle, *Clim. Dyn.*, *20*, 257–267.

Ruth, U., D. Wagenbach, J. P. Steffensen, and M. Bigler (2003), Continuous record of microparticle concentration and size distribution in the central Greenland NGRIP ice core during the last glacial period, *J. Geophys. Res.*, *108*(D3), 4098, doi:10.1029/2002JD002376.

Sánchez Goñi, M. F., I. Cacho, J.-L. Turon, J. Guiot, F. J. Sierro, J.-P. Peypouquet, J. O. Grimalt, and N. J. Shackleton (2002), Synchroneity between marine and terrestrial responses to millennial scale climatic variability during the last glacial period in the Mediterranean region, *Clim. Dyn.*, *19*, 95–105.

Shackleton, N. J., M. A. Hall, and E. Vincent (2000), Phase relationships between millennial-scale events 64,000–24,000 years ago, *Paleoceanogaphy*, *15*, 565–569.

Shackleton, N. J., R. G. Fairbanks, T.-C. Chiu, and F. Parrenin (2004), Absolute calibration of the Greenland time scale: Implications for Antarctic time scales and for Δ^{14}C, *Quat. Sci. Rev.*, *23*, 1513–1522.

Takada, H., J. W. Farrington, M. H. Bothner, C. G. Johnson, and B. W. Tripp (1994), Application of molecular markers for the detection of sewage sludge in the deep sea: Linear alkylbenzenes (LABs), coprostanol, and polycyclic aromatic hydrocarbons (PAHs) at the 106 mile disposal site off the eastern United States, *Environ. Sci. Technol.*, *28*, 1062–1072.

Tolosa, I., J. M. Bayona, and J. Albaiges (1996), Aliphatic and polycyclic aromatic hydrocarbons and sulphur/oxygen derivatives in northwestern Mediterranean sediments: Spatial and temporal variability, fluxes and budgets, *Environ. Sci. Technol.*, *30*, 2495–2503.

Vautravers, M., N. J. Shackleton, C. Lopez-Martinez, and J. O. Grimalt (2004), Gulf Stream variability during marine isotope stage 3, *Paleoceanography*, *19*, PA2011, doi:10.1029/2003PA000966.

Vellinga, M., and R. A. Wood (2002), Global climatic impacts of a collapse of the Atlantic thermohaline circulation, *Clim. Change*, *54*, 251–267.

Villanueva, J., J. O. Grimalt, E. Cortijo, L. Vidal, and L. Labeyrie (1997a), A biomarker approach to the organic matter deposited in the North Atlantic during the last climatic cycle, *Geochim. Cosmochim. Acta*, *61*, 4633–4646.

Villanueva, J., C. Pelejero, and J. O. Grimalt (1997b), Clean-up procedures for the unbiased estimation of C37 alkenones sea surface temperatures and terrigenous *n*-alkane inputs in paleoceanography, *J. Chromatogr.*, *757*, 145–151.

Villanueva, J., J. O. Grimalt, L. D. Labeyrie, E. Cortijo, L. Vidal, and J. L. Turon (1998), Precessional forcing of productivity in the North Atlantic Ocean, *Paleoceanography*, *13*, 561–571.

Villanueva, J., E. Calvo, C. Pelejero, J. O. Grimalt, A. Boelaert, and L. Labeyrie (2001), A latitudinal productivity band in the central North Atlantic over the last 270 kyr: An alkenone perspective, *Paleoceanography*, *16*, 617–626.

Voelker, A. H. L., and Workshop Participants (2002), Global distribution of centennial-scale records for marine isotope stage (MIS) 3: A database, *Quat. Sci. Rev.*, *21*, 1185–1212.

Waelbroeck, C., L. Labeyrie, E. Michel, J. C. Duplessy, J. F. McManus, K. Lambeck, E. Balbon, and M. Labracherie (2002), Sea-level and deep water temperature changes derived from benthic foraminifera isotopic records, *Quat. Sci. Rev.*, *21*, 295–305.

Wang, Y. J., H. Cheng, R. L. Edwards, Z. S. An, J. Y. Wu, C.-C. Shen, and J. A. Dorale (2001), A high-resolution absolute-dated late Pleistocene monsoon record from Hulu Cave, China, *Science*, *294*, 2345–2348.

Watts, W. A. (1979), Late Quaternary vegetation of central Appalachia near the New Jersey Coast Plain, *Ecol. Monogr.*, *49*, 427–469.

Watts, W. A. (1980), The late Quaternary vegetation history of the southeastern United States, *Annu. Rev. Ecol. Syst.*, *11*, 387–409.

Yu, B., and J. M. Wallace (2000), The principal mode of interannual variability of the North American monsoon system, *J. Clim.*, *13*, 2794–2800.

Zhang, Z., M. Zhao, H. Lu, and A. M. Faiia (2003), Lower temperature as the main cause of C4 plant declines during the glacial periods on the Chinese Loess Plateau, *Earth Planet. Sci. Lett.*, *214*, 467–481.

_____

J. O. Grimalt and C. López-Martínez, Department of Environmental Chemistry, Instituto de Investigaciones Químicas y Ambientales de Barcelona, Consejo Superior de Investigaciones Científicas, Jordi Girona, E-08034-Barcelona, Catalonia, Spain. (jgoqam@cid.csic.es)

J. Gruetzner, Fachbereich Geowissenschaften, Universität Bremen, Postfach 33 04 40, D-28334 Bremen, Germany. (jgruetzn@allgeo.uni-bremen.de)

B. Hoogakker and I. N. McCave, Godwin Institute for Palaeoclimate Research, Department of Earth Sciences, University of Cambridge, Downing Street, Cambridge CB2 3EQ, UK. (bhoo03@esc.cam.ac.uk; mccave@esc.cam.ac.uk)

M. J. Vautravers, British Antarctic Survey, High Cross, Madingley Road, Cambridge CB3 0ET, UK. (mava@bas.ac.uk)